Clean Technol., Vol. 27, No. 3, September 2021, pp. 217-222

청정소재제품기술

Transparent Black Phosphorus Nanosheet Film for Photoelectrochemical Water Oxidation

Chang-Ho Choi[1,2,*]

[1]Department of Chemical Engineering, Gyeongsang National University
[2]Department of Materials Engineering and Convergence Technology, Gyeongsang National University
501, Jinju-daero, Jinju-si, Gyeongsangnam-do 52828, South Korea

(Received for review June11, 2021; Revision received July 5, 2021; Accepted July 6, 2021)

Abstract

Although monolayer black phosphorus (BP) and few-layer BP nanosheets (NSs) have been extensively studied as promising alternatives to graphene, research has focused primarily on atomically thin-layered BP in an isolated form. In order to realize the practical applications of BP-related devices, a BP film based on continuous networking of few-layer BP NSs should be developed. In this study, a transparent BP film with high quality was fabricated via a vacuum filtration method. An oxygen-free water solvent was used as an exfoliation medium to avoid significant oxidation of the few-layer BP NSs in liquid-phase exfoliation. The exfoliation efficiency from bulk BP to the few-layer BP NSs was estimated at 22%, which is highly efficient for the production of continuous BP film. The characteristics of the high-quality BP film were determined as 98% transparency, minimum oxidation of 18%, structural stability, and an appropriate bandgap of about 1.8 eV as a semiconductor layer. In order to demonstrate the potential of the BP film for photocatalytic activity, we performed photoelectrochemical water oxidation of the transparent BP film. Although its performance should be improved for practical applications, the BP film could function as a photoanode, which offers a new potential semiconductor in water oxidation. We believe that if the BP film is adequately engineered with other catalysts the photocatalytic activity of the BP film will be improved.

Keywords : Black phosphorus, Photoelectrochemical cell, Water oxidation

1. Introduction

Phosphorene, a monolayer of black phosphorus (BP), has recently garnered considerable attention due to its high electron mobility, anisotropic properties, and tunable electronic bandgap [1,2]. The electronic bandgap is tunable by controlling the thickness of BP, ranging from ~ 0.3 eV for bulk BP to ~ 1.5 eV for a layer of phosphorene, and such a tunable bandgap property is beneficial to many applications such as electronics, optoelectronics, battery, and solar cells [3]. A layer of phosphorene or few-layer BP nanosheets (NSs) can be obtained from exfoliation processes such as mechanical cleavage or liquid exfoliation method, where layered bulk BP delaminates into mono or few-layer one [2]. The exfoliated few-layer BP NSs have been investigated to identify their physical, chemical, thermal, and optical characteristics, which enables to provide valuable scientific insight on potential applications of layered BP [1,4-6].

Aside from devices based on the exfoliated BP NSs, the continuous BP film, formed by the connected few-layer BP NSs, should be developed for their practical applications in a wide range of research areas. There are a few reports regarding the preparation of BP film, including drop-casting of BP NSs dispersion on the substrate and phase conversion of red phosphorus (RP) film into BP counterpart under high pressure [7]. Although these methods enabled to formation of the continuous BP film, there remain some issues in establishing high-uniformity and controlled film thickness. In particular, the phase conversion approach suffers an inherent process complexity associated with the high pressure. On the other hand, a vacuum filtration method is facile in preparing a 2D material film on various substrates and allows the fabrication of free-standing (substrate-free) film as well [8-10].

In this study, we report the fabrication of the continuous and transparent BP film via the vacuum filtration method. Various

* To whom correspondence should be addressed.
E-mail: ch_choi@gnu.ac.kr; Tel: +82-55-772-1781; Fax: +82-55-772-1789

doi: 10.7464/ksct.2021.27.3.217 pISSN 1598-9712 eISSN 2288-0690

characterizations of the BP film were conducted to study its morphological, optical, and chemical properties. Additionally, the photocatalytic activity of the BP film was evaluated by a photoelectrochemical (PEC) water oxidation reaction of the film.

2. Material and methods

2.1. Exfoliation of powder BP into few-layer BP nanosheets

Bulk BP was purchased from Smart Elements. 5 mg of bulk BP was ground to powder and transported into a glass vial containing 20 mL of oxygen-free water. The oxygen-free water was obtained by purging Ar gas into D.I. water solvent for at least 0.5 h. The transport of the bulk BP powder and sealing of the vial were carried out in Ar glove box (Jisico, J-924D) to avoid any contamination or degradation of bulk BP. The BP powder in the vial was immersed in ultrasonic bath and subject to ultrasound for 12 h at room temperature. The temperature of the bath was maintained through a chiller, and exfoliation conditions were maintained with 40 KHz and output power of 350 W. The exfoliated BP NPs were separated from unexfoliated BP by centrifugation (Gyrozen, 1236MG) at 4,000 rpm for 20 min.

2.2. Fabrication of BP film by vacuum-filtration method

A dispersion of the exfoliated BP NSs was transported onto a cellulose acetate membrane (Advantec, 200 nm pore size) using the vacuum-filtration apparatus. After the filtration, the stacked BP nanosheets on the membrane was placed in a vacuum oven for 2 h at 80 ℃ to evaporate the water solvent. The membrane was then put on the substrate upside down, followed by immersing in N-Methyl-2-pyrrolidone (NMP) solvent to remove the membrane.

2.3. Characterization

Thickness and lateral size of the exfoliated BP NSs were examined by an atomic force microscopy (AFM). The AFM was performed with a PSIA (XE-100) in a tapping mode, and scanned images were analyzed by a XEI software. For the AFM sample preparation, 0.1 mL of supernatant containing the exfoliated BP NSs was transported onto the SiO_2 (100 nm)/Si substrate and dried in a vacuum oven at 80 ℃ for 6 h to evaporate the solvent. Optical properties of the exfoliated BP dispersion were studied by UV-Vis spectroscopy (Thermo Scientific, NanoDrop 2000). The crystallinity and purity of the exfoliated BP NSs were examined by high-resolution transmission electron microscopy (HRTEM, JEOL JEM-2100F), fast Fourier transform (FFT), and energy-dispersive X-ray spectroscopy (EDS). The HRTEM was operated at 200 kV. For the preparation of the HRTEM specimen, 10 μL of the supernatant was dripped on a lacey carbon grid (Ted Pella) and dried in a vacuum oven at 80 ℃ for 6 h. The dried specimen was stored in an Ar glove box.

Morphology and thickness of the BP film were characterized by high-resolution FE-SEM (JSM 7800F PRIME). Crystallinity of the BP film was analyzed by X-ray-diffractometer (XRD, Rigaku Max-2500) with Cu Kα radiation (acceleration voltage: 40 kV, flux: 40 mA). Elemental composition of the BP film was studied by X-ray photoelectron spectroscopy (XPS, ESCALAB 200-IXL instrument with Mg K radiation). Raman scattering was carried out on a Horiba XploRa Plus Raman spectrometer equipped with 532 nm laser as the excitation source at room temperature. The specimen for the Raman scattering analysis was prepared in the same manner for the AFM analysis. Optical properties of the BP film were conducted by UV-Vis-NIR spectroscopy (Jasco, V-670).

2.4. Exfoliation efficiency estimation of few-layer BP nanosheet

After the centrifugation, a supernatant containing the exfoliated BP NSs was carefully decanted, and unexfoliated BP was re-dispersed into water solvent. The re-dispersed BP was collected onto a cellulose acetate membrane (Advantec, 200 nm pore size) under the vacuum filtration system and dried in a vacuum oven at 120 ℃ for 24 h to completely remove the water solvent. The weight of the bare membrane and the BP membrane was measured five times in an Ar glove box by using a fine scale (4-digit decimal point, Ohaus Pioneer) for the precise weight measurement. The exfoliation efficiency of the few-layer BP NSs was estimated as follows.

$$\text{Exfoliation efficiency (\%)} = \text{exfoliated BP amount/initial BP amount} \times 100$$

3. Results and Discussion

In order to fabricate the continuous BP film, the few-layer BP NSs should be obtained from bulk BP through an exfoliation process. In our experiment, the exfoliation process was carried out in an ultrasonic bath for 12 h using oxygen-free water as the exfoliation solvent. The use of the oxygen-free water is very critical to obtain high-quality BP NSs because oxygen is a major cause to facilitate the degradation of BP NSs [11,12]. A recent study also supports the use of oxygen-free water is necessary to produce the few-layer BP NSs with high purity in an aqueous phase [13]. Figure 1 shows the characteristics of the exfoliated few-layer BP NSs. The exfoliation process and subsequent centrifugation (4,000 rpm for 20 min) led to the production of the few-layer BP NSs, with an exfoliation efficiency of 22% (0.06 mg mL^{-1}). The exfoliated BP dispersion exhibits the broad absorption spectrum at visible wavelengths, consistent with reported

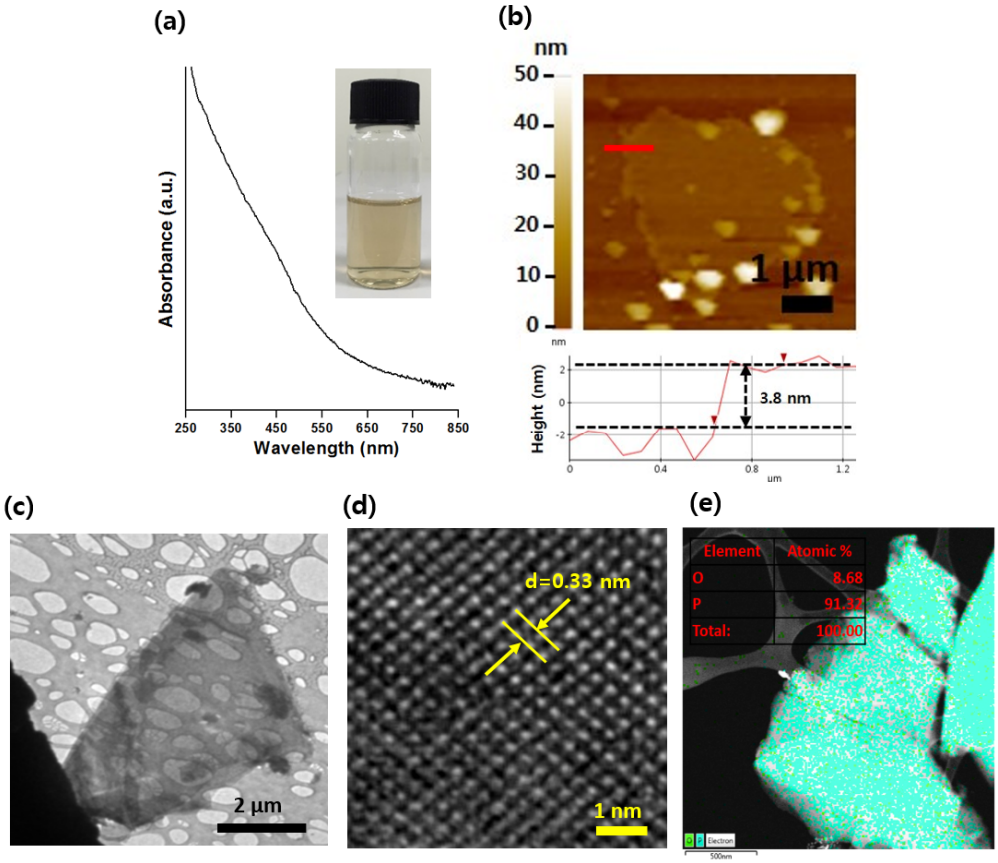

Figure 1. Characteristics of the few-layer BP NSs exfoliated in oxygen-free water: (a) UV-Vis absorption (inset: optical image of the BP dispersion), (b) AFM image with a thickness profile, (c) a representative TEM, (d) HRTEM image, and (e) EDS mapping image of BP NS.

few-layer BP NSs (Figure 1(a)) [14]. A typical few-layer BP NS shows 3.8 nm and 4 μm in the thickness and lateral size, respectively, according to the AFM analysis (Figure 1(b)). The thickness corresponds to 4 ~ 5 layers of phosphorene, and the lateral dimension is large enough to be filtered onto a membrane (200 nm pore size) during the vacuum filtration process [15]. The TEM and HRTEM images confirm the high crystallinity of the few-layer BP NS with the clear lattice fringe (Figure 1(c) and (d)). The EDS elemental analysis presents the atomic composition of the BP NS with 91% phosphorus and 9% oxygen atom (Figure 1(e)). These characteristic results indicate that the few-layer BP NSs exfoliated in oxygen-free water are eligible for the building blocks to constitute the continuous BP film.

The BP dispersion containing the few-layer BP NSs was subject to the vacuum-filtration process for the fabrication of the BP film. The vacuum-filtration process has several advantages in forming the continuous BP film with high uniformity [7,8]. As the BP dispersion was poured onto the membrane, the micron-sized BP NSs were accumulated on the membrane while those smaller than the membrane pore size (200 nm) passed through the membrane. The thickness of the BP film could be self-regulated because the permeation degree of the BP dispersion depends on the accumulation degree of the BP NSs on the membrane [8]. Therefore, simply varying the concentration of the BP NSs, the thickness of the BP film can be tuned in nanoscale. The BP film on the membrane could be translated on the FTO glass by gently pressing the front side of the BP film on the FTO glass, followed by the dissolution of the membrane in an acetone solvent. The optical image in Figure 2(a) displays the BP film with a circular shape (2 cm in diameter). A 5 mL BP dispersion containing ~ 0.3 mg BP NSs was used to prepare the film. It seems that the translation process of the BP film from the membrane to FTO glass did not create any noticeable structural damage. The film showed light yellowish color and high transparency. Some fractions of the BP film were composed of wrinkled structures according to the plain SEM image, and the cross-sectional SEM view shows the uniform BP film with the thickness of 98 ± 16 nm (Figure 2(b) and (c)). The sharp peaks in the XRD spectrum indicate the high crystallinity of the BP film, and its XRD patterns are perfectly matched with the reference (Figure 2(d)) [16]. One may speculate that the BP film could further degrade during the vacuum filtration process. To clarify this, we conducted the XPS analysis and investigated the chemical composition of the BP film (Figure 2(e)). Three distinct peaks at 129.7, 130.4, and 133.6 eV

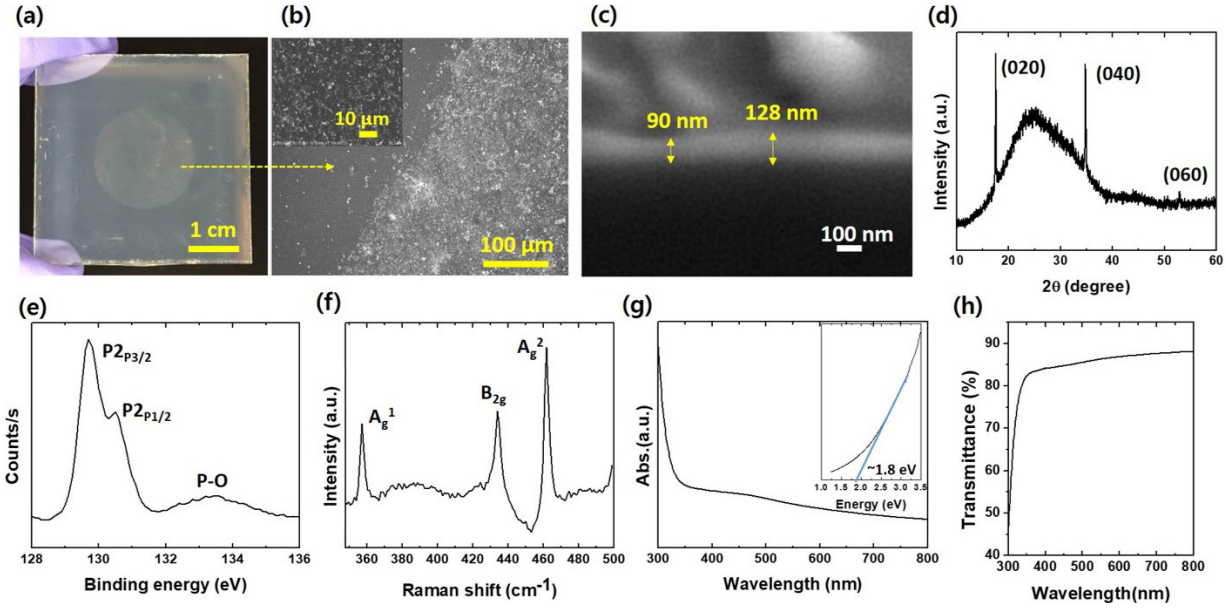

Figure 2. Characterizations of the BP film prepared by vacuum-filtration method: (a) optical image of the BP film on FTO substrate, (b) plain view SEM image, (c) cross-sectional view SEM image, (d) XRD spectroscopy, (e) XPS spectroscopy, (f) Raman spectroscopy, (g) absorption spectrum (inset: bandgap measurement), and (h) transmittance spectrum.

were detected, assigned to $P2_{p3/2}$, $P2_{p1/2}$, and P_xO_y, respectively [17]. The peaks of $P2_{p3/2}$ and $P2_{p1/2}$ correspond to pure phosphorus, while the peak at 133.6 eV is attributed to the oxidation of phosphorus. The quantification of the peak fitting revealed that the BP film degrades in 18% oxidation, reflecting that the few-layer BP NSs further degraded during the vacuum-filtration process. However, the major component of the film was still pure phosphorus, and according to the Raman scattering analysis, its structural as well as chemical properties were well retained (Figure 2(f)). Three strong peaks appeared at 363.2, 440, and 467.8 cm^{-1}, corresponding to the A_{g^1}, B_{2g}, and A_{g^2} modes of BP, respectively [18]. Compared to the bulk BP, all the peaks shifted to higher wavenumber, commonly observed from the few-layer BP NSs [6]. Lastly, the optical properties of the BP film were studied by the absorption and transmittance spectra. The broad absorption peak at visible wavelengths was observed from the BP film (Figure 2(g)). The Tauc plot presents the estimated bandgap of the film with ~ 1.8 eV, complying with monolayer or few-layer BP NSs [19]. A 86% transmittance at 600 nm wavelength was obtained for the BP film, demonstrating its high transparency (Figure 2(h)).

Studies on photocatalytic activity of BP have shown that bandgap and energy alignment of few-layer BP NSs are suitable for both oxidation and reduction of water [20]. For example, the BP NSs led to hydrogen production in a much high yield, as compared to red phosphorus nanoparticles in the presence of platinum (Pt) [21]. Photocatalytic activity of a ZIF-8/BP nanocomposite was also more effective in degrading methylene blue (MB) than homogeneous ZIF and BP NSs does [22]. The BP NSs decorated with silver (Ag) nanoparticles demonstrated the enhanced photocatalytic activity in decomposing rhodamine B (Rh B), as compared to pristine BP NSs [23]. These studies are associated with pristine BP NSs or hybrid BP NSs, but the BP film as a photoelectrode has not been reported. The successful fabrication of the continuous BP film via the vacuum filtration method enabled us to apply the BP film for photoelectrode.

PEC oxidation of water on BP film was investigated with linear sweep voltammograms (LSVs) in a solution of 0.1 M potassium phosphate buffer (KPi, pH 7) under chopped light illumination (AM 1.5G, 100 mW cm^{-2}) (Figure 3(a)). BP film exhibited electrocatalytic (EC) activity for oxygen evolving reaction (OER) with the onset potential of at 1.7 V_{RHE}. The photocurrent onset potential of the BP film was at 0.61 V_{RHE}, more negative than EC activity. These results indicate that the BP film can function as a photoanode even if its photocurrent activity is insufficient to generate oxygen detectable by GC instrument (capacity of HPLC). At a constant potential of 1.6 V_{RHE}, the BP film exhibited a sharp peak photocurrent promptly upon the light irradiation, followed by a stable photocurrent with 1.8 μA cm^{-2} within tens of seconds (Figure 3(b)). The peak photocurrent may be attributed to the fast charge recombination of the BP NSs on the film. The stable photocurrent of the BP film sustained without any noticeable reduction, implying the long-term stability of BP film in the experimental conditions. Zhao et al. [21] also reported the long-term stability of the BP NSs up to 96 hr for hydrogen production in water under light irradiation. The BP film, composed of the connected BP NSs, would likely resist against degradation due to the role of the topmost BP layer that serves as

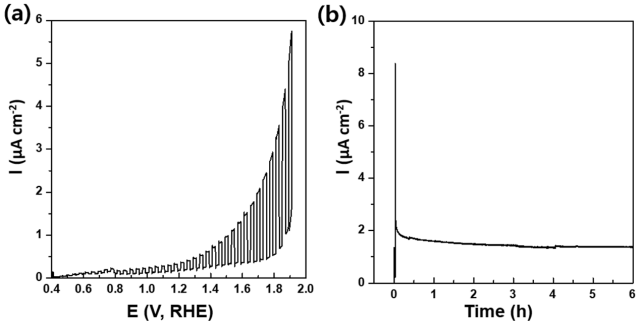

Figure 3. Photocatalytic water oxidation results of the BP film: (a) LSVs under chopped light illumination (AM 1.5G, 100 $mWcm^{-2}$) and (b) photocurrent generation at 1.6 VRHE under light illumination up to 6 h.

passivation [24].

The PEC water oxidation of the BP film demonstrates that BP has a suitable valence band edge for the water oxidation and could be a potential semiconductor as a photoanode. However, the photocatalytic activity of the BP film should be further improved for its practical application. In order to enhance its photocatalytic performances, engineering the BP film is urgently needed to suppress the recombination of electrons and holes and efficiently transfer the charge carriers. The improved performance may be achieved by forming a heterojunction with other semiconductors such as TiO_2 and WO_3, depositing co-catalyst, and employing appropriate passivation layers.

4. Conclusions

The BP NSs were produced in oxygen-free water exfoliation with exfoliation efficiency of 22%. The high-quality BP NSs were used to fabricate the continuous BP film via the vacuum filtration method. The characteristics of the continuous BP film were elucidated including the morphological, optical, chemical, and structural properties. All of these characteristic results demonstrated the high-quality of the BP film that is suitable for a photoanode in PEC water oxidation. BP film exhibited electrocatalytic activity for OER with the onset potential of at 1.7 V_{RHE}, and its photocurrent onset potential was at 0.61 V_{RHE}, more negative than EC activity. This study paves the way for the potential applications of the continuous BP film in photocatalytic water splitting.

Acknowledgement

This work was supported by a National Research Foundation of Korea (NRF) grant funded by the Korea government (No. 2019R1I1A3A01058865) and (NRF-2019H1D8A210599).

References

1. Liu, H., Du, Y., Deng, Y., and Ye, P. D., "Semiconducting Black Phosphorus: Synthesis, Transport Properties and Electronic Applications," *Chem. Soc. Rev.*, **44**(9), 2732-2743 (2015).
2. Liu, H., Neal, A. T., Zhu, Z., Luo, Z., Xu, X., Tománek, D., and Ye, P. D., "Phosphorene: An Unexplored 2D Semiconductor with a High Hole Mobility," *ACS Nano*, **8**(4), 4033-4041 (2014).
3. Kou, L., Chen, C., and Smith, S. C., "Phosphorene: Fabrication, Properties, and Applications," *J. Phys. Chem. Lett.*, **6**(14), 2794-2805 (2015).
4. Castellanos-Gomez, A., Vicarelli, L., Prada, E., Island, J. O., Narasimha-Acharya, K. L., Blanter, S. I., Groenendijk, D. J., Buscema, M., Steele, G. A., and Alvarez, J. V., "Isolation and Characterization of Few-Layer Black Phosphorus," *2D Mater.*, **1**(2), 025001 (2014).
5. Xu, J.-Y., Gao, L.-F., Hu, C.-X., Zhu, Z.-Y., Zhao, M., Wang, Q., and Zhang, H.-L., "Preparation of Large Size, Few-Layer Black Phosphorus Nanosheets Via Phytic Acid-Assisted Liquid Exfoliation," *Chem. Commun.*, **52**(52), 8107-8110 (2016).
6. Brent, J. R., Savjani, N., Lewis, E. A., Haigh, S. J., Lewis, D. J., and O'Brien, P., "Production of Few-Layer Phosphorene by Liquid Exfoliation of Black Phosphorus," *Chem. Commun.*, **50**(87), 13338-13341 (2014).
7. Li, X., Deng, B., Wang, X., Chen, S., Vaisman, M., Karato, S.-I., Pan, G., Lee, M. L., Cha, J., Wang, H., and Xia, F., "Synthesis of Thin-Film Black Phosphorus on a Flexible Substrate," *2D Mater.*, **2**(3), 031002 (2015).
8. Eda, G., Fanchini, G., and Chhowalla, M., "Large-area Ultrathin Films of Reduced Graphene Oxide as a Transparent and Flexible Electronic Material," *Nat. Nanotechnol*, **3**(5), 270-274 (2008).
9. Wu, Z., Chen, Z., Du, X., Logan, J. M., Sippel, J., Nikolou, M., Kamaras, K., Reynolds, J. R., Tanner, D. B., Hebard, A. F., and Rinzler A. G., "Transparent, Conductive Carbon Nanotube Films," *Science*, **305**(5688), 1273-1276 (2004).
10. Dikin, D. A., Stankovich, S., Zimney, E. J., Piner, R. D., Dommett, G. H., Evmenenko, G., Nguyen, S. T., and Ruoff, R. S., "Preparation and Characterization of Graphene Oxide Paper," *Nature*, **448**(7152), 457-460 (2007).
11. Favron, A., Gaufrès, E., Fossard, F., Phaneuf-L'Heureux, A.-L., Tang, N. Y., Lévesque, P. L., Loiseau, A., Leonelli, R., Francoeur, S., and Martel, R., "Photooxidation and Quantum Confinement Effects in Exfoliated Black Phosphorus," *Nat. Mater.*, **14**(8), 826-832 (2015).
12. Wang, G., Slough, W. J., Pandey, R., and Karna, S. P., "Degradation of Phosphorene in Air: Understanding at Atomic Level," *2D Mater.*, **3**(2), 025011 (2016).

13. Wang, H., Yang, X., Shao, W., Chen, S., Xie, J., Zhang, X., Wang, J., and Xie, Y., "Ultrathin Black Phosphorus Nanosheets for Efficient Singlet Oxygen Generation," *J. Am. Chem. Soc.*, **137**(35), 11376-11382 (2015).
14. Guo, Z., Zhang, H., Lu, S., Wang, Z., Tang, S., Shao, J., Sun, Z., Xie, H., Wang, H., Yu, X.-F., and Chu, P. K., "From Black Phosphorus to Phosphorene: Basic Solvent Exfoliation, Evolution of Raman Scattering, and Applications to Ultrafast Photonics," *Adv. Funct. Mater.*, **25**(45), 6996-7002 (2015).
15. Deng, Y., Luo, Z., Conrad, N. J., Liu, H., Gong, Y., Najmaei, S., Ajayan, P. M., Lou, J., Xu, X., and Ye, P. D., "Black Phosphorus-Monolayer MoS_2 Van Der Waals Heterojunction p-n Diode," *ACS Nano*, **8**(8), 8292-8299 (2014).
16. Chen, L., Zhou, G., Liu, Z., Ma, X., Chen, J., Zhang, Z., Ma, X., Li, F., Cheng, H.-M., and Ren, W., "Scalable Clean Exfoliation of High-Quality Few-Layer Black Phosphorus for a Flexible Lithium Ion Battery," *Adv. Mater.*, **28**(3), 510-517 (2016).
17. Kang, J., Wood, J. D., Wells, S. A., Lee, J. H., Liu, X., Chen, K. S., and Hersam, M. C., "Solvent Exfoliation of Electronic-Grade, Two-Dimensional Black Phosphorus," *ACS Nano*, **9**(4), 3596-3604 (2015).
18. Hanlon, D., Backes, C., Doherty, E., Cucinotta, C. S., Berner, N. C., Boland, C., Lee, K., Harvey, A., Lynch, P., Gholamvand, Z., Zhang, S., Wang, K., Moynihan, G., Pokle, A., Ramasse, Q. M., McEvoy, N., Blau, W. J., Wang, J., Abellan, G., Hauke, F., Hirsch, A., Sanvito, S., O'Regan, D. D., Duesberg, G. S., Nicolosi, V., and Coleman, J. N., "Liquid Exfoliation of Solvent-Stabilized Few-Layer Black Phosphorus for Applications Beyond Electronics," *Nat. Commun.*, **6**(1), 8563 (2015).
19. Liu, Y., Qiu, Z., Carvalho, A., Bao, Y., Xu, H., Tan, S. J. R., Liu, W., Neto, A. H. C., Loh, K. P., and Lu, J., "Gate-Tunable Giant Stark Effect in Few-Layer Black Phosphorus," *Nano Lett.*, **17**(3), 1970-1977 (2017).
20. Rahman, M. Z., Kwong, C. W., Davey, K., Qiao, S. Z., "2D Phosphorene as a Water Splitting Photocatalyst: Fundamentals to Applications," *Energ. Environ. Sci.*, **9**(3), 709-728 (2016).
21. Zhao, G., Wang, T., Shao, Y., Wu, Y., Huang, B., and Hao, X., "A Novel Mild Phase-Transition to Prepare Black Phosphorus Nanosheets with Excellent Energy Applications," *Small*, **13**(7), 1602243 (2017).
22. Wang, L., Xu, Q., Xu, J., and Weng, J., "Synthesis of Hybrid Nanocomposites of ZIF-8 with Two-Dimensional Black Phosphorus for Photocatalysis," *Rsc Adv.*, **6**(73), 69033-69039 (2016).
23. Lei, W., Zhang, T., Liu, P., Rodriguez, J. A., Liu, G., and Liu, M., "Bandgap- and Local Field-Dependent Photoactivity of Ag/Black Phosphorus Nanohybrids," *ACS Catal.*, **6**(12), 8009-8020 (2016).
24. Zhou, Q., Chen, Q., Tong, Y., and Wang, J., "Light-induced Ambient Degradation of Few-Layer Black Phosphorus: Mechanism and Protection," *Angew. Chem. Int. Ed.*, **55**(38), 11437-11441 (2016).